Research Article

Puja Basu Chaudhuri, Anirban Mitra, and Sarmila Sahoo*

Mode frequency analysis of antisymmetric angle-ply laminated composite stiffened hypar shell with cutout

https://doi.org/10.2478/mme-2019-0022
Received Nov 02, 2017; revised May 10, 2018; accepted Nov 20, 2018

Abstract: This article deals with finite element method for the analysis of antisymmetric angle-ply laminated composite hypar shells (hyperbolic paraboloid bounded by straight edges) that applies an eight-noded isoparametric shell element and a three-noded beam element to study the mode-frequency analysis of stiffened shell with cutout. Two-, 4-, and 10-layered antisymmetric angle-ply laminations with different lamination angles are considered. Among these, 10-layer antisymmetric angle-ply shells are considered for elaborate study. The shells have different boundary conditions along its four edges. The formulation is based on the first-order shear deformation theory. The reduced method of eigen value solution is chosen for the undamped free vibration analysis. The first five modes of natural frequency are presented. The numerical studies are conducted to determine the effects of width-to-thickness ratio (b/h), degree of orthotropy (E_{11}/E_{22}), and fiber orientation angle (θ) on the nondimensional natural frequency. The results reveal that free vibration behavior mainly depends on the number of boundary constraints rather than other parametric variations such as change in fiber orientation angle and increase in degree of orthotropy and width-to-thickness ratio.

Keywords: stiffened hypar shell, cutout, anti-symmetric angle-ply composite, finite element method, mode-frequency analysis

***Corresponding Author: Sarmila Sahoo:** Department of Civil Engineering, Heritage Institute of Technology, Kolkata 700107, India; Email: sarmila.sahoo@gmail.com
Puja Basu Chaudhuri: Department of Civil Engineering, Heritage Institute of Technology, Kolkata 700107, India
Anirban Mitra: Department of Mechanical Engineering, Jadavpur University, Kolkata 700032, India

1 Introduction

Laminated composite shells now constitute a large percentage of structures including aerospace, marine, and automotive structural components. Structural engineers have already picked up laminated composite hypar shells (hyperbolic paraboloid bounded by straight edges) as roofing units because these can cover large column-free areas with reduced dead weight. This class of shells has only the radius of cross curvature that is unique to this shell form. Roof structures are sometimes provided with cutout to allow the entry of light, venting and to provide the accessibility of parts of the structures, and also to alter the resonant frequency. Shells with cutout stiffened along the margin are an efficient way to enhance the stiffness of the structure without adding much mass. These stiffeners slightly increase the overall weight of the structure but have positive effect on the structural strength and stability. So to apprehend the laminated composite stiffened hypar shells with cutout and to use this shell form efficiently, its characteristics under vibration need to be explored comprehensively.

The subject of laminated shells has attracted several researchers during the past decade. Considerable attention has been paid to dynamic analyses, including free vibration, impact, transient, shock, etc. From the review of literature, it is observed that shell research has been conducted with emphasis on complicating effects in material such as damping and piezoelectric behavior and complicated structures such as stiffened shells with cutout with various boundary conditions. Applications of various shell theories such as classical, shear deformation, 3D, and nonlinear for various shell geometries have received extensive attention from scholars round the globe [1–8]. Some studies used higher order shell theories [9–16], whereas others [17–23] considered finite element approach based on the first-order shear deformation theory to study the free vibration aspects of stiffened shell panels of different forms, that is, cylindrical, elliptic paraboloid, hyperbolic paraboloid, hypar, conoid, and spherical shells in the pres-

ence of cutout. But the analysis of stiffened shells with cutout for higher modes is scanty in the literature. Some studies [24, 25] also reported the mode frequency analysis of laminated spherical and cylindrical shells. However, the analysis of stiffened hypar shells with cutout for higher modes is yet to be reported in literature. Hence, an attempt has been made in the present article to provide some information about the effects of width-to-thickness ratio (b/h), degree of orthotropy (E_{11}/E_{22}), and fiber orientation (θ) on the nondimensional natural frequency for antisymmetric angle-ply hypar shells with 10-layer laminates in the presence of cutout and stiffeners for different practical boundary conditions.

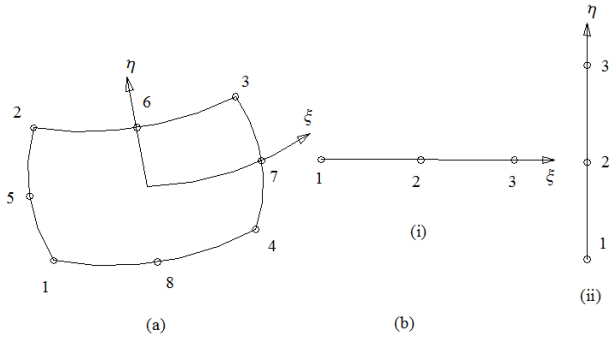

Figure 2: (a) Eight-noded shell element. (b) Three-noded stiffener element: (i) *X*-stiffener and (ii) *Y*-stiffener

2 Mathematical Formulation

A laminated composite hypar shell of uniform thickness h (Figure 1) and twist radius of curvature R_{xy} is considered. The shell thickness may consist of any number of thin laminae each of which may be arbitrarily oriented at an angle θ with reference to the X-axis of the coordinate system. An eight-noded, curved, quadratic, isoparametric, finite element (Figure 2a) is used. The five degrees of freedom taken into consideration at each node include two in-plane and one transverse displacement and two rotations about the X- and Y-axes. The strain–displacement and constitutive relationships together with the systematic development of stiffness matrix for the shell element has been reported earlier [7] and the same is used in the present case as well.

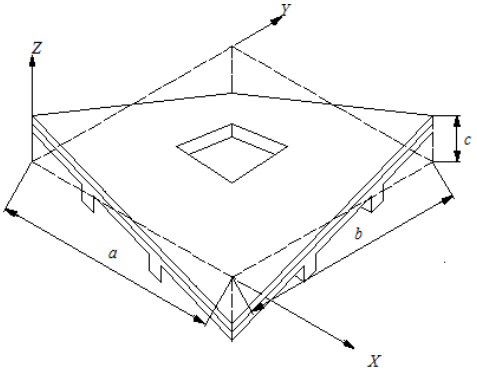

Figure 1: Surface of a skewed hypar shell with cutout

Three-noded isoparametric beam elements (Figure 2b) are used to model the stiffeners, which are taken to run only along the boundaries of the shell elements. In the stiffener element, each node has four degrees of freedom, that is, u_{sx}, w_{sx}, α_{sx}, and β_{sx} for X-stiffener and v_{sy}, w_{sy}, α_{sy}, and β_{sy} for Y-stiffener. The generalized force–displacement relation of stiffeners can be expressed as follows (the notations have been defined in Appendix A):

$$\begin{aligned} &X - \text{stiffener}: \{F_{sx}\} = [D_{sx}]\{\varepsilon_{sx}\} \\ &= [D_{sx}][B_{sx}]\{\delta_{sxi}\}; \\ &Y - \text{stiffener}: \{F_{sy}\} = [D_{sy}]\{\varepsilon_{sy}\} = [D_{sy}][B_{sy}]\{\delta_{syi}\} \end{aligned} \tag{1}$$

where

$$\{F_{sx}\} = \begin{bmatrix} N_{sxx} & M_{sxx} & T_{sxx} & Q_{sxxz} \end{bmatrix}^T;$$

$$\{\varepsilon_{sx}\} = \begin{bmatrix} u_{sx.x} & \alpha_{sx.x} & \beta_{sx.x} & (\alpha_{sx} + w_{sx.x}) \end{bmatrix}^T$$

and

$$\{F_{sy}\} = \begin{bmatrix} N_{syy} & M_{syy} & T_{syy} & Q_{syyz} \end{bmatrix}^T;$$

$$\{\varepsilon_{sy}\} = \begin{bmatrix} v_{sy.y} & \beta_{sy.y} & \alpha_{sy.y} & (\beta_{sy} + w_{sy.y}) \end{bmatrix}^T.$$

Elasticity matrices are expressed as follows:

$$[D_{sx}] = \begin{bmatrix} A_{11}b_{sx} & B'_{11}b_{sx} & B'_{12}b_{sx} & 0 \\ B'_{11}b_{sx} & D'_{11}b_{sx} & D'_{12}b_{sx} & 0 \\ B'_{12}b_{sx} & D'_{12}b_{sx} & \frac{1}{6}(Q_{44}+Q_{66})d_{sx}b_{sx}^3 & 0 \\ 0 & 0 & 0 & b_{sx}S_{11} \end{bmatrix}$$

$$[D_{sy}] = \begin{bmatrix} A_{22}b_{sy} & B'_{22}b_{sy} & B'_{12}b_{sy} & 0 \\ B'_{22}b_{sy} & \frac{1}{6}(Q_{44}+Q_{66})b_{sy} & D'_{12}b_{sy} & 0 \\ B'_{12}b_{sy} & D'_{12}b_{sy} & D'_{11}d_{sy}b_{sy}^3 & 0 \\ 0 & 0 & 0 & b_{sy}S_{22} \end{bmatrix},$$

where

$$D'_{ij} = D_{ij} + 2eB_{ij} + e^2A_{ij} \tag{2}$$

and A_{ij}, B_{ij}, D_{ij}, and S_{ij} are explained in an earlier paper [7].

Here the shear correction factor is taken as 5/6. The sectional parameters are calculated with respect to the mid-surface of the shell by which the effect of eccentricities of stiffeners is automatically included. The element stiffness matrices are of the following forms.

$$\text{for } X-\text{stiffener}: [K_{xe}] = \int [B_{sx}]^T [D_{sx}] [B_{sx}]\, dx; \quad (3)$$
$$\text{for } Y-\text{stiffener}: [K_{ye}] = \int [B_{sy}]^T [D_{sy}] [B_{sy}]\, dy.$$

The integrals are converted to isoparametric coordinates and are carried out by 2 point Gauss quadrature. Finally, the element stiffness matrix of the stiffened shell is obtained by appropriate matching of the nodes of the stiffener and shell elements through the connectivity matrix and is written as follows:

$$[K_e] = [K_{she}] + [K_{xe}] + [K_{ye}] \quad (4)$$

The element stiffness matrices are assembled to get the global matrices.

The element mass matrix for shell is obtained from the following integral equation:

$$[M_e] = {}^T [P] [N]\, dxdy \quad (5)$$

where

$$[N] = \sum_{i=1}^{8} \begin{bmatrix} N_i & 0 & 0 & 0 & 0 \\ 0 & N_i & 0 & 0 & 0 \\ 0 & 0 & N_i & 0 & 0 \\ 0 & 0 & 0 & N_i & 0 \\ 0 & 0 & 0 & 0 & N_i \end{bmatrix},$$

$$[P] = \sum_{i=1}^{8} \begin{bmatrix} P & 0 & 0 & 0 & 0 \\ 0 & P & 0 & 0 & 0 \\ 0 & 0 & P & 0 & 0 \\ 0 & 0 & 0 & I & 0 \\ 0 & 0 & 0 & 0 & I \end{bmatrix},$$

in which

$$P = \sum_{k=1}^{np} \int_{z_{k-1}}^{z_k} \rho dz \text{ and } I = \sum_{k=1}^{np} \int_{z_{k-1}}^{z_k} z\rho dz \quad (6)$$

Element mass matrix for the stiffener element is

$$[M_{sx}] = {}^T [P] [N]\, dx \quad \text{for } X-\text{stiffener} \quad (7)$$
$$\text{and } [M_{sy}] = {}^T [P] [N]\, dy \quad \text{for } Y-\text{stiffener}.$$

Here, $[N]$ is a 3×3 diagonal matrix.

$[P] =$

$$\sum_{i=1}^{3} \begin{bmatrix} \rho.b_{sx}d_{sx} & 0 & 0 & 0 \\ 0 & \rho.b_{sx}d_{sx} & 0 & 0 \\ 0 & 0 & \rho.b_{sx}d_{sx}^2/12 & 0 \\ 0 & 0 & 0 & \rho(b_{sx}.d_{sx}^3 + b_{sx}^3.d_{sx})/12 \end{bmatrix}$$

for X – stiffener,

$[P] =$

$$\sum_{i=1}^{3} \begin{bmatrix} \rho.b_{sy}d_{sy} & 0 & 0 & 0 \\ 0 & \rho.b_{sy}d_{sy} & 0 & 0 \\ 0 & 0 & \rho.b_{sy}d_{sy}^2/12 & 0 \\ 0 & 0 & 0 & \rho(b_{sy}.d_{sy}^3 + b_{sy}^3.d_{sy})/12 \end{bmatrix}$$

for Y–stiffener.

The mass matrix of the stiffened shell element is the sum of the matrices of the shell and the stiffeners matched at the appropriate nodes.

$$[M_e] = [M_{she}] + [M_{xe}] + [M_{ye}] \quad (8)$$

The element mass matrices are assembled to get the global matrices.

In regards to the modeling of the cutout, the code developed can take the position and size of cutout as input. The program is capable of generating nonuniformal finite element mesh all over the shell surface. So the element size is gradually decreased near the cutout margins. One such typical mesh arrangement is shown in Figure 3. Such finite element mesh is redefined in steps and a particular grid is chosen to obtain the fundamental frequency when the result does not improve by more than 1% on further refining. Convergence of results is ensured in all the problems taken up here.

Finally, the free vibration analysis involves the determination of natural frequencies from the condition

$$\left| [K] - \omega^2 [M] \right| = 0 \quad (9)$$

This is a generalized eigen value problem and is solved by the subspace iteration algorithm.

3 Numerical Examples

Problems are solved with two different objectives. Benchmark problems are used to check the suitability of the present approach and a number of authors' own problems are taken up to assess the mode–frequency behavior of antisymmetric angle-ply composite stiffened hypar shells with cutout.

The accuracy of the present formulation is first validated by comparing the results of the following problems

Table 1: Natural frequencies (*Hz*) of centrally stiffened clamped square plate

Mode no.	Mukherjee and Mukhopadhyay [26]	Nayak and Bandyopadhyay [4]		Present method
		N8 (FEM)	N9 (FEM)	
1	711.8	725.2	725.1	733

$a = b = 0.2032$ m; thickness = 0.0013716 m; stiffener depth = 0.0127 m; stiffener width = 0.00635 m; stiffener eccentric at bottom. Material property: $E = 6.87 \times 10^{10}$ N/m^2, $\nu = 0.29$, $\rho = 2{,}823$ kg/m^3

Table 2: Nondimensional fundamental frequencies ($\bar{\omega}$) for hypar shells (lamination $(0/90)_4$) with concentric cutouts

a'/a	Chakravorty et al. [1])		Present finite element model					
	Simply supported	Clamped	Simply supported			Clamped		
			8 × 8	10 × 10	12 × 12	8 × 8	10 × 10	12 × 12
0.0	50.829	111.600	50.573	50.821	50.825	111.445	111.592	111.612
0.1	50.769	110.166	50.679	50.758	50.779	109.987	110.057	110.233
0.2	50.434	105.464	50.323	50.421	50.400	105.265	105.444	105.443
0.3	49.165	101.350	49.045	49.157	49.178	101.110	101.340	101.490
0.4	47.244	97.987	47.132	47.242	47.141	97.670	97.985	97.991

$a/b = 1$; $a/h = 100$; $a'/b' = 1$; $c/a = 0.2$; $E_{11}/E_{22} = 25$; $G_{23} = 0.2\,E_{22}$; $G_{13} = G_{12} = 0.5\,E_{22}$; $\nu_{12} = \nu_{21} = 0.25$.

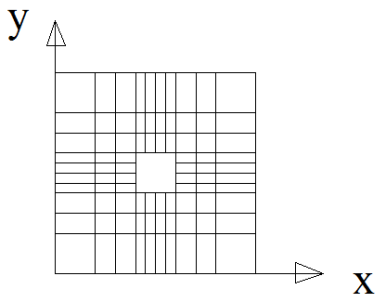

Figure 3: Typical 10 × 10 nonuniformal mesh arrangement drawn to scale

available in the existing literature. The results presented in Table 1 show that the agreement of the present results with the earlier ones [4, 26] is excellent and the correctness of the stiffener formulation is established. Free vibration of simply supported and clamped hypar shell having $(0/90)_4$ lamination and with cutouts is also considered. The fundamental frequencies of hypar shell with cutout obtained by the present method agree well with those reported by Chakravorty *et al.* [1], which is evident from Table 2, establishing the correctness of the cutout formulation. Thus it is evident that the finite element model proposed here can successfully analyze vibration problems of stiffened skewed hypar composite shells with cutout that is reflected by a close agreement of the present results with benchmark ones.

Antisymmetric angle-ply laminated composite stiffened hypar shells with cutout are analyzed to study the behavior of the shell under free vibration at higher mode for different parametric variation. The cutouts are placed concentrically on the shell surface. The stiffeners are placed along the cutout periphery and extended up to the edge of the shell. The material and geometric properties of the shells are $a/b = 1$, $a/h = 100$, $a'/b' = 1$, $a'/a = 0.2$, $c/a = 0.2$, $E_{11}/E_{22} = 25$, $G_{23} = 0.2\,E_{22}$, $G_{13} = G_{12} = 0.5\,E_{22}$, $\nu_{12} = \nu_{21} = 0.25$, and $\rho = 100$ N-s^2/m^4 unless otherwise specified.

Seven laminated stacking sequences, namely, antisymmetric angle-ply $(0/-0)_{10}$, $(15/-15)_{10}$, $(30/-30)_{10}$, $(45/-45)_{10}$, $(60/-60)_{10}$, $(75/-75)_{10}$, and $(90/-90)_{10}$ are considered. Numerical analyses are performed to determine the effect of fiber orientation angle ($\theta = 0°$, 15°, 30°, 45°, 60°, 75°, and 90°), degree of orthotropy ($E_{11}/E_{22} = 5$, 10, 20, 25, 30, 40, and 50), and width-to-thickness ratio ($b/h =$ 10, 20, 50, 100) on nondimensional natural frequency.

The different boundary conditions that are used in the present analysis are CSCS, CSSC, FCCF, FCFC, FSFS and FSSF. The boundary conditions are designated as: C for clamped, S for simply supported, and F for free edges. The four edges are considered in an anticlockwise order starting from the edge $x = 0$. For example, a shell with CSCS boundary is clamped along $x = 0$, simply supported along $y = 0$, clamped along $x = a$, and simply supported along $y = b$.

4 Results and Discussion

Table 3 presents the nondimensional fundamental frequency (the first-mode frequencies) for 2-, 4-, and 10-

Table 3: Nondimensional fundamental frequency of antisymmetric angle-ply multilayered laminated composite stiffened hypar shell with cutout

Angle-ply	Boundary Condition	Two Layers	Four Layers	Ten Layers
0°	CSCS	6.356	6.356	6.356
15°		6.056	7.467	7.892
30°		6.787	9.399	10.121
45°		7.825	11.356	12.324
60°		8.914	12.622	13.631
75°		10.196	12.919	13.642*
90°		13.254*	13.254*	13.254
0°	CSSC	13.017	13.016	13.016
15°		12.449	13.979	14.307
30°		12.607	14.954	15.547
45°		13.356*	15.369*	15.799*
60°		12.526	14.928	15.549
75°		12.402	13.998	14.362
90°		13.008	13.008	13.008
0°	FCCF	6.539	6.539	6.539
15°		6.011	6.855	7.082
30°		6.263	7.327*	7.555*
45°		6.233	7.161	7.377
60°		6.196	7.212	7.436
75°		6.000	6.806	7.024
90°		6.548*	6.548	6.548
0°	FCFC	11.707*	11.706*	11.708*
15°		8.031	10.746	11.394
30°		5.875	8.628	9.246
45°		4.283	6.033	6.435
60°		3.147	3.795	3.958
75°		2.674	2.741	2.759
90°		2.604	2.604	2.604
0°	FSFS	4.367*	4.367	4.367
15°		4.041	4.732	4.882
30°		3.974	4.984*	5.204*
45°		2.941	4.038	4.293
60°		2.194	2.583	2.679
75°		1.860	1.905	1.918
90°		1.806	1.806	1.806
0°	FSSF	3.628*	3.628	3.628
15°		3.310	3.945	4.127
30°		3.349	4.190*	4.403*
45°		3.290	4.166	4.380
60°		3.304	4.104	4.307
75°		3.268	3.860	4.027
90°		3.560	3.560	3.560

layered antisymmetric angle-ply laminated composite stiffened hypar shells with cutout with the fiber orientation angle varying between 0° and 90°. In each column, the maximum value is indicated by an asterisk. It is observed that for the two-layered hypar shell, maximum fundamental frequency occurs at the lamination angle of either 0° or 90° except for CSSC shell. For CSSC shell, the maximum fundamental frequency occurs at the lamination angle of 45°. It is also observed that for all the boundary conditions considered here, 4- and 10-layered laminates exhibit the maximum value of frequency parameter for the same lamination angle., The maximum fundamental frequency occurs at the lamination angle, θ, of 75° and 45°, respectively, for CSCS and CSSC shells; at $\theta = 0°$ for FCFC shells; and at $\theta = 30°$ for FCCF, FSFS and FSSF shells. This observation is valid for both 4- and 10-layered hypar shells. According to the number of boundary constraints, boundary conditions can be grouped as CSCS & CSSC; FCCF & FCFC; and FSFS & FSSF. For all the layers considered here, as the number of boundary constraint increases, the fundamental frequency increases. Thus CSCS & CSSC perform better than FCCF & FCFC, which in turn perform better than FSFS & FSSF shells. It is also observed from Table 3 that with the increase in layer, the frequency parameter increases. The increments are sharper from 2 to 4 layers compared to 4 to 10 layers, in which a mild increase in the frequency parameter is observed. As the 10-layered laminates exhibit best performance, so far the fundamental frequency is concerned, they are considered for further studies.

4.1 Effect of fiber orientation

The total thickness of the laminate was maintained constant, and the number of layers is 10. Figure 4 shows the variation of nondimensional frequency with boundary

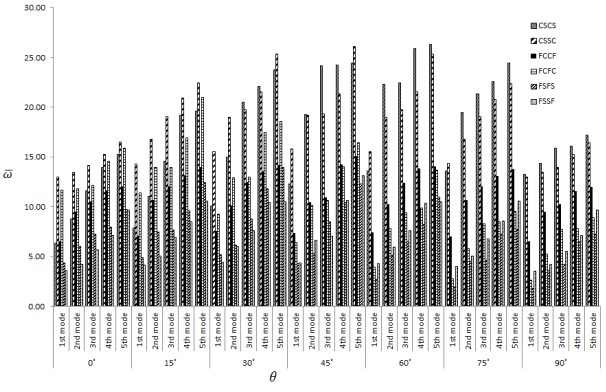

Figure 4: Variation of nondimensional fundamental frequency with the fiber orientation angle

conditions and lamination angle. Seven laminate stacking sequences, namely, antisymmetric angle-ply $(0/-0)_{10}$, $(15/-15)_{10}$, $(30/-30)_{10}$, $(45/-45)_{10}$, $(60/-60)_{10}$, $(75/-75)_{10}$, and $(90/-90)_{10}$ are considered. The nondimensional frequency parameter for the first, second, third, fourth, and fifth mode increases with an increase in the fiber orientation angle from 0° to 45° for CSSC, FCCF, and FSFS shells, but further increase in the lamination angle decreases the fundamental frequency. Similarly, for CSCS shell, the fundamental frequency increases up to 60° and then decreases. Again for FCFC shell, fundamental frequency decreases with an increase in the lamination angle. On the other hand for FSSF shell, the change in the frequency with change in lamination angle is very insignificant. For all the laminations and boundary conditions considered here, frequency parameter increases from the first mode to the fifth mode except in few cases in which frequency parameter is almost the same in two consecutive modes. The lamination and boundary conditions interact in a complex manner so that no unified conclusion can be reached. The reason behind this is that the frequencies depend on the contribution made by extensional stiffness, coupling stiffness, and bending stiffness terms in addition to the boundary conditions and panel geometry, among others. However, for all the lamination angles considered here, CSCS & CSSC perform better than FCCF & FCFC, which in turn perform better than FSFS & FSSF. So it can be concluded that the number of boundary constraints plays a great role for free vibration. CSSC performs better than CSCS for lower lamination angles, but for higher lamination angle, CSCS performs better than CSSC. But reverse trend is observed when free edges are involved. FCFC and FSFS perform better in lower lamination angle but FCCF and FSSF perform better in higher lamination angle.

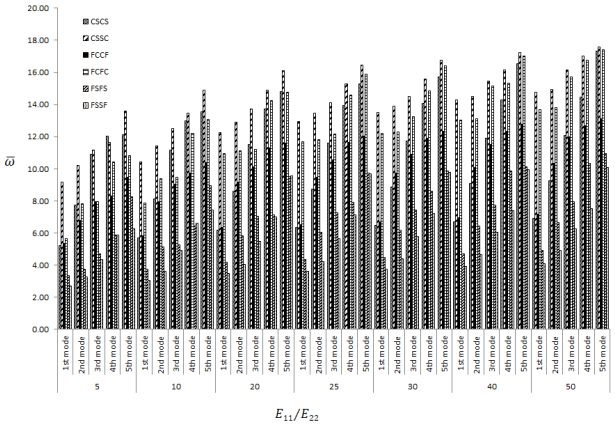

Figure 5: Variation of nondimensional fundamental frequency with material anisotropy for $(0/-0)_{10}$ lamination

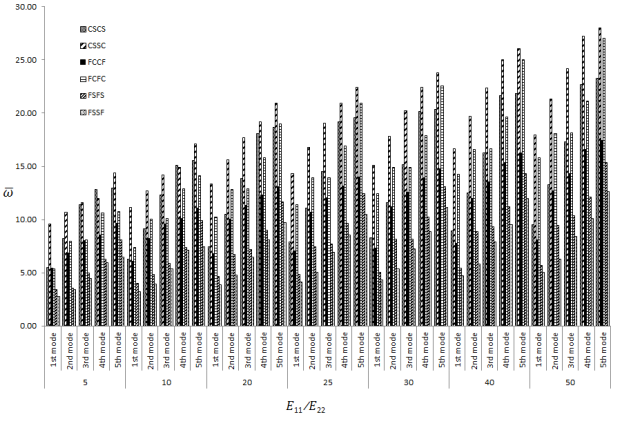

Figure 6: Variation of nondimensional fundamental frequency with material anisotropy for $(15/-15)_{10}$ lamination

4.2 Effect of material anisotropy

The effects of material anisotropy on the frequencies of 10-layer antisymmetric angle-ply square shells with fiber orientation angles of 0°, 15°, 30°, 45°, 60°, 75°, and 90° for CSCS, CSSC, FCCF, FCFC, FSFS, and FSSF edge boundary conditions, respectively, are demonstrated in Figures 5–11.

These results are obtained by keeping the material properties as constant, that is, $G_{12}/E_{22} = 0.5$ and $\nu_{12} = 0.25$, and changing the E_{11}/E_{22} ratio. As observed from these figures, as the degree of orthotropy increases, the first, second, third, fourth, and fifth frequency parameter increases monotonically for all the laminations and boundary conditions considered here. These increments are sharper for CSSC shell. FCFC shell shows better performance for lower

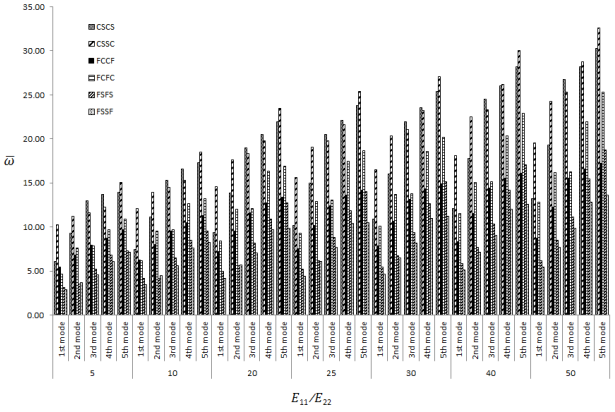

Figure 7: Variation of nondimensional fundamental frequency with material anisotropy for $(30/-30)_{10}$ lamination

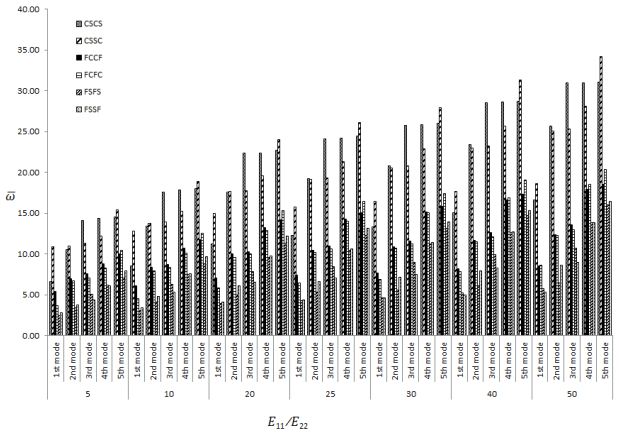

Figure 8: Variation of nondimensional fundamental frequency with material anisotropy for $(45/-45)_{10}$ lamination

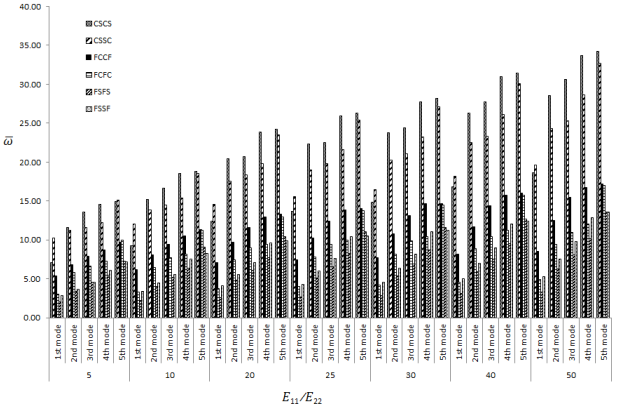

Figure 9: Variation of non-dimensional fundamental frequency with material anisotropy for $(60/-60)_{10}$ lamination

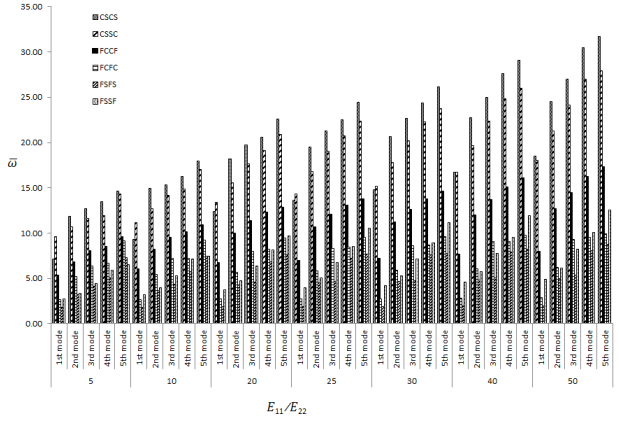

Figure 10: Variation of nondimensional fundamental frequency with material anisotropy for $(75/-75)_{10}$ lamination

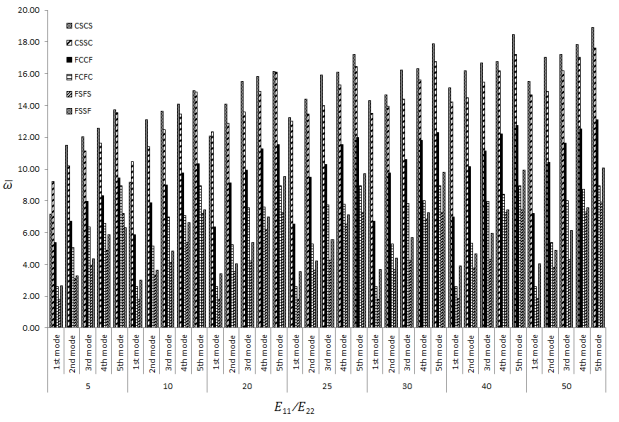

Figure 11: Variation of nondimensional fundamental frequency with material anisotropy for $(90/-90)_{10}$ lamination

lamination angle, but with the increase in the lamination angle, the performance of CSCS shell is better. For other boundary conditions, mild increase in the frequency parameter is observed. It is also observed that for almost all the cases, the frequency parameter increases from the first mode to the fifth mode. In a few cases, the frequency remains almost same between two consecutive modes.

4.3 Effect of width-to-thickness ratio

If the width-to-thickness ratio is increased while maintaining the width of the laminate a constant and the number of layers being fixed at 10, the thickness of the shell is decreased. Figures 12–18 show the variation of the nondimensional frequency for the first, second, third, fourth and fifth mode with variation of width-to-thickness ratio and boundary conditions for various values of lamination angles. Ten-layer antisymmetric angle-ply laminates with

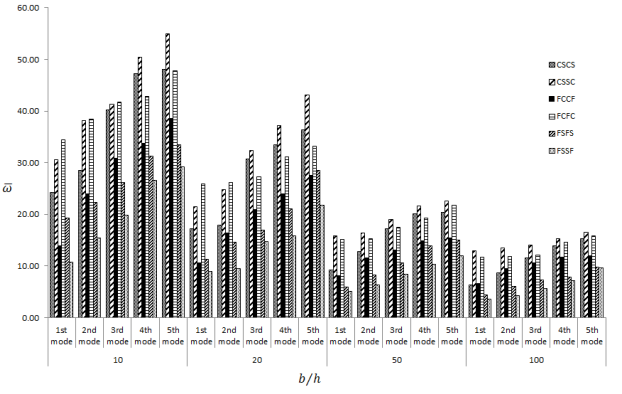

Figure 12: Variation of nondimensional fundamental frequency with b/h ratio for $(0/-0)_{10}$ lamination

varying fiber orientation angle, such as 0°, 15°, 30°, 45°, 60°, 75°, and 90°, having different width-to-thickness ratios (b/h = 10, 20, 50, 100) are analyzed. It is evident from Figures 12–18 that with the increase in width-to-thickness ratio, the dimensionless frequencies decrease. This decrease in frequency is very much significant in case of CSSC, CSCS, and FCFC shells. For other boundary conditions, this decrease in dimensionless frequency is signifi-

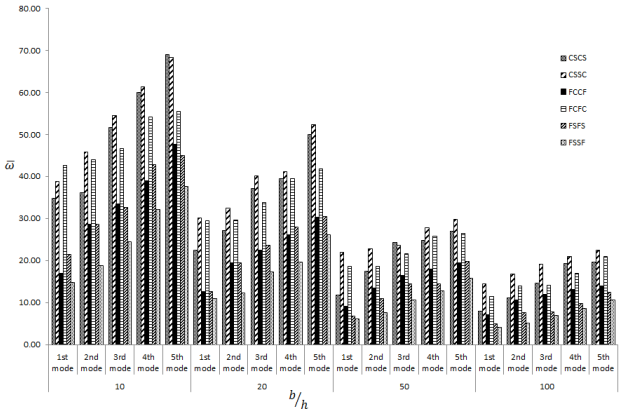

Figure 13: Variation of non-dimensional fundamental frequency with b/h ratio for $(15/-15)_{10}$ lamination

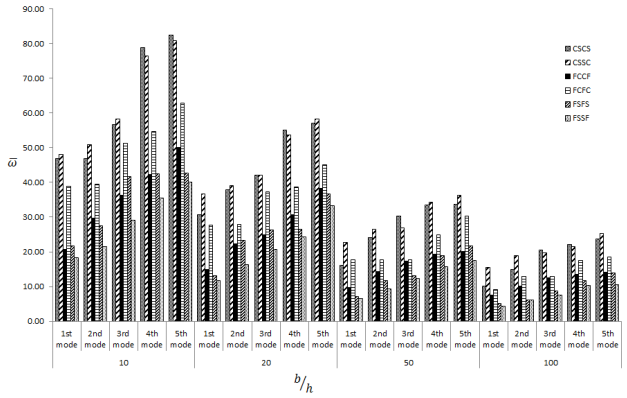

Figure 14: Variation of nondimensional fundamental frequency with b/h ratio for $(30/-30)_{10}$ lamination

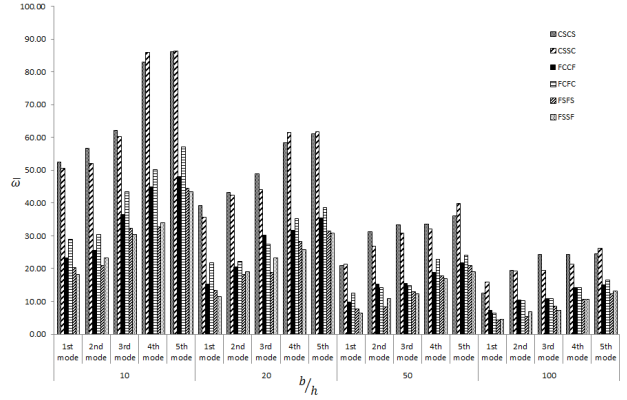

Figure 15: Variation of nondimensional fundamental frequency with b/h ratio for $(45/-45)_{10}$ lamination

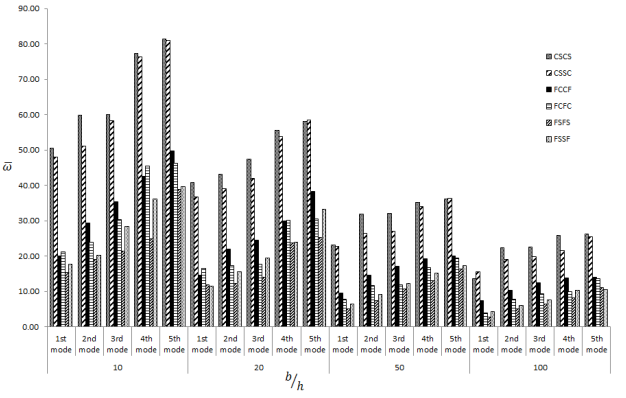

Figure 16: Variation of nondimensional fundamental frequency with b/h ratio for $(60/-60)_{10}$ lamination

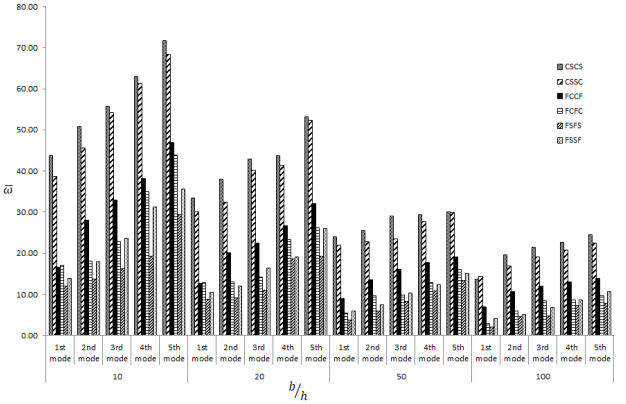

Figure 17: Variation of nondimensional fundamental frequency with b/h ratio for $(75/-75)_{10}$ lamination

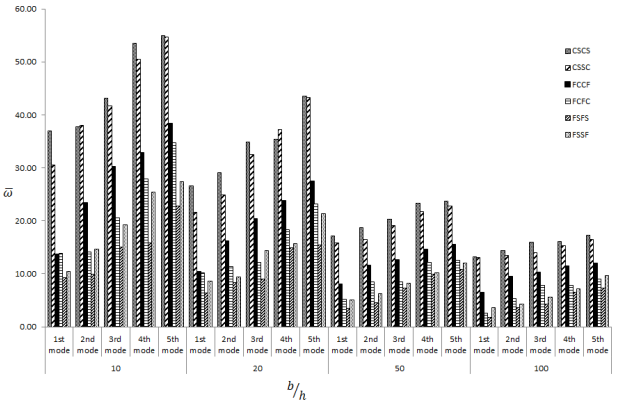

Figure 18: Variation of nondimensional fundamental frequency with b/h ratio for $(90/-90)_{10}$ lamination

cant at higher value of width-to-thickness ratio. These are true for all the five modes. Here also for all the combination of stacking sequences, boundary conditions, and width-to-thickness ratios, the nondimensional frequency increases from the first mode to the fifth mode except few cases.

5 Conclusions

In this article, analysis of antisymmetric angle-ply laminated composite stiffened hypar shell with cutout is presented for different modes of vibration using finite element method based on the first-order shear deformation theory. It can be concluded by analyzing the results that as the number of layers increase, the fundamental frequency increases. With the increase in lamination angle, nondimensional natural frequency may increase or decrease, but from the first mode to the fifth mode, natural frequency always increase or remain same in very few cases. The first, second, third, fourth, and fifth nondimensional frequency parameter increases monotonically for all the laminations and boundary conditions as the degree of orthotropy increases. With the increase in width-to-thickness ratios, dimensionless frequencies decrease from the first mode to the fifth mode. Free vibration behavior mainly depends on the number of boundary constraints whatever may be the other parametric variations such as change in fiber orientation angle and increase in the degree of orthotropy and width-to-thickness ratio.

Nomenclature

ν_{12}, ν_{21}	Poisson's ratios
ω	natural frequency
$\overline{\omega}$	nondimensional natural frequency = $\omega\, a^2 \left(\rho/E_{22}h^2\right)^{1/2}$
ρ	density of material
E_{11}, E_{22}	elastic moduli
G_{12}, G_{13}, G_{23}	shear moduli of a lamina with respect to 1, 2 and 3 axes of fiber
α_{sx}, β_{sx}	rotational degrees of freedom at each node of X-stiffener element
α_{sy}, β_{sy}	rotational degrees of freedom at each node of Y-stiffener element
δ_{sxi} , δ_{syi}	nodal displacement of stiffener element
a', b'	length and width of cutout in plan
B_{sx}, B_{sy}	strain displacement matrix of stiffener element
M_{sxx}, M_{syy}	moment resultants of stiffeners
N_{sxx}, N_{syy}	axial force resultants of stiffeners
Q_{sxxz}, Q_{syyz}	transverse shear resultants of stiffeners
T_{sxx}, T_{syy}	torsion resultants of stiffeners
a ,b	length and width of shell in plan
b_{sx}, b_{sy}	width of X and Y stiffeners, respectively
c	rise of hypar shell
d_{sx}, d_{sy}	depth of X and Y stiffeners, respectively
e_{sx}, e_{sy}	eccentricities of X and Y stiffeners with respect to mid surface of shell
e	eccentricity of stiffeners with respect to mid surface of shell
h	shell thickness
np	number of plies in a laminate
R_{xy}	radii of cross curvature of hypar shell
u_{sx}, w_{sx}	axial and transverse translational degrees of freedom at each node of X-stiffener element
v_{sy}, w_{sy}	axial and transverse translational degrees of freedom at each node of Y-stiffener element
X, Y, Z	global coordinate axes
x, y, z	local coordinate axes
z_k	distance of bottom of the k-th ply from mid-surface of a laminate

References

[1] Chakravorty, D., Bandyopadhyay, J.N., Sinha, P.K.: Applications of FEM on free and forced vibrations of laminated shells, ASCE J. Engg. Mech.,124(1), 1–8, 1998.

[2] Rikards R., Chate A., Ozolinsh O.: Analysis for buckling and vibrations of composite stiffened shells and plates, Composite Struct.,51, 361–370, 2001.

[3] Nayak, A.N., Bandyopadhyay, J.N.: Free vibration analysis and design aids of stiffened conoidal shells, ASCE J. Engg. Mech.,128(4), 419–427, 2002.

[4] Nayak, A.N., Bandyopadhyay, J.N.: On the free vibration of stiffened shallow shells, J. Sound and Vibr.,255(2), 357–382, 2002.

[5] Nayak, A.N., Bandyopadhyay, J.N.: Free vibration analysis of laminated stiffened shells. ASCE J. Engg. Mech., 131(1), 100–105, 2005.

[6] Nayak, A.N., Bandyopadhyay, J.N.: Dynamic response analysis of stiffened conoidal shells,J. Sound and Vibr.,291, 1288-1297, 2006.

[7] Sahoo, S., Chakravorty, D.: Finite element vibration characteristics of composite hypar shallow shells with various edge supports, J. Vibr. Control,11, 1291–1309, 2005.

[8] Sahoo, S., Chakravorty, D.: Stiffened composite hypar shell roofs under free vibration: behaviour and optimization aids. J. Sound and Vibr.,295, 362-377, 2006.

[9] Pradyumna, S., Bandyopadhyay, J.N.: Free vibration analysis of functionally graded curved panels using a higher order finite

element formulation, J. Sound and Vibr.,318, 176-192, 2008.
[10] Kumar, A., Bhargava, P., Chakrabarti, A.: Natural Frequencies and mode shape of laminated composite skew hypar shells with complicated boundary conditions using finite element method, Adv. Mat. Res., 585, 44-48, 2012.
[11] Kumar, A., Bhargava, P., Chakrabarti, A.: Vibration of laminated composite skew hypar shells using higher order theory, Thin Walled Structures,63, 82-90, 2013.
[12] Kumar, A., Chakrabarti, A., Bhargava, P.: Vibration analysis of laminated composite skew cylindrical shells using higher order shear deformation theory, J. Vib. Control,21(4), 725-735, 2015.
[13] GulshanTaj, M.N.A., Chakraborty, A.: Dynamic response of functionally graded skew shell panel, Latin Amer. J. Solids Struct.,10, 1243-1266, 2013.
[14] Tornabene, F., Fantuzzi, N., Bacciocchi, M., Dimitri, R.: Dynamic analysis of thick and thin elliptic shell structures made of laminated composite materials, Compos. Struct.,133, 278-299, 2015.
[15] Dey, S., Mukhopadhyay, T., Adhikari, S.: Stochastic free vibration analyses of composite shallow doubly curved shells-A Kriging model approach, Composite: Part B, 70, 99-112, 2015.
[16] Zhang, C., Jin G., Ma, X., Ye, T.: Vibration analysis of circular cylindrical double-shell structures under general coupling and end boundary conditions, Appl. Acoustics, 110, 176-193, 2016.
[17] Sahoo, S.: Behaviour and optimization aids of composite stiffened hypar shell roofs with cutout under free vibration, ISRN Civil Engg., ID 989785, 1-14, 2012.
[18] Sahoo, S.: Dynamic characters of stiffened composite conoidal shell roofs with cutouts: Design aids and selection guidelines, J. Engg., ID 230120, 1-18, 2013.
[19] Sahoo, S.: Free vibration of laminated composite stiffened saddle shell roofs with cutouts, IOSR J. Mech. Civil Engg., ICAET, 30-34, 2014.
[20] Sahoo, S.: Laminated composite stiffened shallow spherical panels with cutouts under free vibration – a finite element approach, Engg. Sci. Tech., An Int. J.,17(4), 247-259, 2014.
[21] Sahoo, S.: Free vibration behavior of laminated composite stiffened elliptic paraboloidal shell panel with cutout, Curved and Layered Struct.,2(1), 162-182, 2015.
[22] Sahoo, S.: Laminated composite stiffened cylindrical shell panels with cutouts under free vibration, Int. J. Manuf. Mat. Mech.Engg.,5(3), 37-63, 2015.
[23] Sahoo, S.: Performance evaluation of free vibration of laminated composite stiffened hyperbolic paraboloid shell panel with cutout, Int. J. Engg. Technol.,7, 1-24, 2016.
[24] Topal, U.: Mode-frequency analysis of laminated spherical shell, Proceedings of the 2006 IJME. INTERTECH International Conference-Session ENG P501-001, Kean University, NJ; 19-21 October 2006.
[25] Srinivasa, C.V., Suresh Y.J., Prema Kumar, W.P.: Experimental and finite element studies on free vibration of cylindrical skew panels, Int. J. Advanced Struct. Engg., 6(1), 1-11, 2014.
[26] Mukherjee, A., Mukhopadhyay, M.: Finite element free vibration of eccentrically stiffened plates, Comp. Struct., 30, 1303-1317, 1988.